DOI: 10.3901/CJME.2013.02.393, available online at www.springerlink.com; www.cjmenet.com; www.cjmenet.com.cn

Sawing Performance Comparison of Brazed and Sintered Diamond Wires

HUANG Guoqin* and XU Xipeng

Engineering Research Center of Brittle Materials Machining of Ministry of Education, Huaqiao University, Xiamen 361021, China

Received May 31, 2012; revised October 10, 2012; accepted November 15, 2012

Abstract: Great attention has been paid on fabricating diamond wire by using the brazing diamond because of its strong chemical bonding strength and controllability of grits distribution. Although several serving performances of brazed diamond wire have been reported, seldom do these studies refer to its process characteristics. Sawing performances of a brazed diamond wire are investigated and compared with those of a sintered diamond wire on a wire saw machine. The surface topographies of beads selected from the two wires are micro observed before sawing. The sawing tests are carried out in constant feed rate feeding(CFF) and constant normal force feeding(CNFF). In CFF test, sawing force, power, and the cut depths of positions on contact curve are measured. Then, coupled with the observations of beads topographies, sawing force and its ratio, relations of power against material removal rate, and contact curve linearity are compared and discussed. In CNFF test, the sawing rates of the two wires are investigated. The results indicate that the brazed wire performs with lower sawing force(less 16% of tangential force and 28% of normal force), more energy efficiency(nearly one-fifth of sawing power is saved), at a higher sawing rate (the rate is doubled) and with better contact curve linearity as compared with the sintered wire. This proposed research experimentally evaluates the sawing performances of brazed diamond wire from the aspect of process parameters, which can provide a basis for popularizing the brazed diamond wire.

Keywords: diamond wire, braze, sinter, sawing force, power, contact curve

1 Introduction

In recent decades, diamond wire saws have played an important role in the processing of natural stone, removing large structures (huge buildings, railway bridges, old concrete chimneys and dams) and cutting cables and oil pipes below the sea surface[1–3]. These diamond wire saws are employed in such a variety of circumstances because of their high flexibility, high production rate, low noise level, low cost and high energy efficiency, particularly when compared to circular saws[4].

The basic model of the diamond wire sawing is shown Fig. 1. In general, a diamond wire is a steel cable on which small diamond beads are mounted at regular intervals with a spacing tube cover placed between adjacent beads. The diamond wire is connected into an endless circle and tensed on a wheel system. The wheel system consists of a drive, slave and guide wheels and tensioning structures. Each of diamond beads at the wire/workpiece contact curve firmly presses onto the workpiece because of the inner tensions of wire. When the wire is driven at a high tangential speed (wire speed), the diamond grits held on the beads execute the cutting action. The entire cutting operation greatly depends on the wire speed (v_s), feed rate (v_f), sawing length (L) and wire tension (T_0).

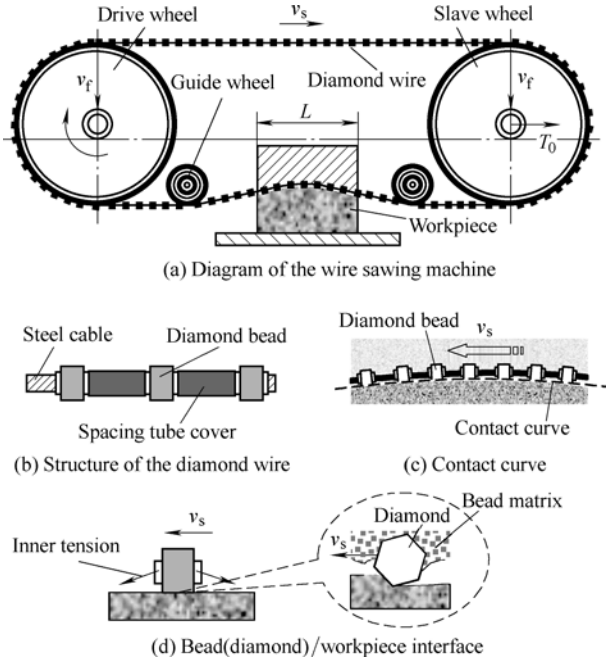

Fig. 1. Basic model of the diamond wire sawing

It is obvious that the beads are the most important part of

* Corresponding author. E-mail: smarthgq@hqu.edu.cn

This project is supported by National Natural Science Foundation of China(Grant Nos. 51235004, 51105148, 51175194), and Program for Changjiang Scholars and Innovative Research Team in University of China(Grant No. IRT1063)

the diamond wire because they are responsible for the material removing action. For any diamond abrasive tool, holding the diamond grits on the tool's matrix is vital. Over the past decades, the powder metallurgy sintering has been widely used in processing diamond beads[5]. However, as diamonds are very difficult to wet, they are only mechanically held on the bead matrix because there is no chemical bonding realised at the diamond/matrix interface. Therefore, the bonding strength is poor. Together with the severe chip slurry friction at the wire/workpiece interface, the diamond pull-off from the bead matrix is a serious wear flaw in using sintered diamond wire saws[6–9]. To improve the diamond retention on the beads, OLIVEIRA, et al[10] developed a new metal matrix system with the aim of improving the bonding strength of diamonds. RISSO, et al[11] designed an innovative shape for beads to reduce grit wear. ÖZÇELIK[12–13] investigated the optimal cutting conditions of diamond wire and developed a device to investigate its wear. Although many efforts have been undertaken to improve the bonding strength, little has been achieved because chemical reactions at the diamond/matrix (active brazing alloys) interface are perhaps impossible by these two ways.

In the early 1990s, the success of brazing diamonds onto a steel substrate opened a new era in manufacturing diamond tools[14]. Because of the strong chemical bonding provided by the carbide formation at the diamond/active alloys interface and the success of placing grits in a predetermined pattern, the brazed diamond tools could cut much faster and significantly longer than the conventional tools[15]. In 1999, SUNG[16] introduced the brazing technique into the processing of diamond beads. Because of the outstanding outcomes exhibited by the brazed diamond wire, as reported by SUNG[16] and XIAO, et al[17], the brazed diamond was considered as a revolutionary design to the diamond wire processing. However, all these reports focused mainly on sawing efficiency, tool wear resistance and service life. Few studies covered force, contact curve and energy consumption. In this study, this situation is remedied by investigating the effect of a variety of parameters on the forces, energy consumption, contact curve and the sawing efficiency of a brazed wire and the results are compared with a commercially available sintered wire.

2 Experimental Details

2.1 Setup of the sawing platform

The comparative work is conducted by using a small wire saw with a wire length varying between 5.3 m and 5.5 m. The setup of the wire saw measuring system is illustrated in Fig. 2. The resultant of sawing forces distributing on the wire/workpiece contact curve can be decomposed into tangential force (F_t) and normal force (F_n) along the tangential and the normal directions of the contact curve, respectively. On the basis of the workpiece coordinate system, this resultant also can be decomposed into horizontal and vertical forces (F_h and F_v, respectively). In this work, F_h and F_v are measured by a Kistler 9257BA dynamometer. The power(P) is monitored by a GX-3 power meter. Signals of the forces and power are sampled at a frequency of 1 kHz by using a DEWE-2010 data acquisition system. All these signals are low-pass filtered with a cut-off frequency of 100 Hz. Typical filtered signals are shown in Fig. 3. Each net value induced by the sawing action is obtained by subtracting the average value in the idling stage (without cut) from that in the steady sawing stage(with cut).

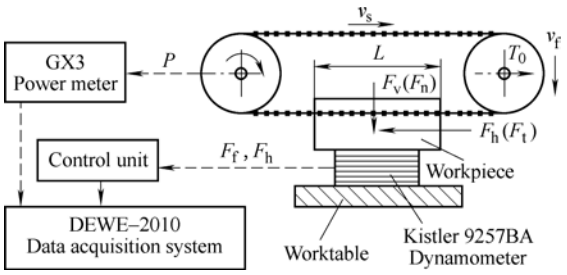

Fig. 2. Wire saw mesusuring system setup

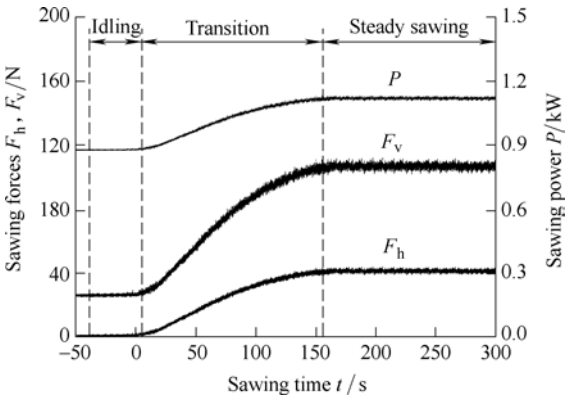

Fig. 3. Typical filtered signals

As shown in Fig. 4, a constant pressure feeding table is built to realise a constant normal force feeding mode when investigating the sawing efficiency. The normal force can be loaded and adjusted by a weight.

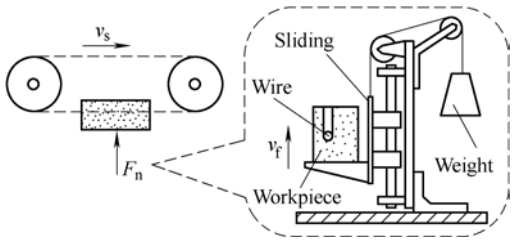

Fig. 4. Constant pressure feeding table

The cut depth(D_c) of point on the different position of the contact curve, which is the vertical distance from the point to the top of the workpiece, is measured by a depth vernier. As shown in Fig. 5, the cut depth of point A is illustrated as D_{c-A} on the figure.

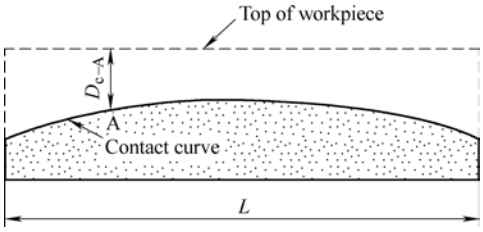

Fig. 5. Cut depth on the contact curve

2.2 Observation of bead surface topography

A digital optical microscope (Hirox KH–1000HI Scope) is employed to inspect the topography of the diamond bead. The protrusive height of grit on the bead (h_p) is measured (see Fig. 6). The ratio of the grit protrusive height to its diameter (d_g) is defined as the grit protrusive rate (λ). The ratio of the average protrusive height of all grits on a bead (h_{pav}) to the average grit diameters (d_{gav}) is defined as the average grit protrusive rate (λ_{av}).

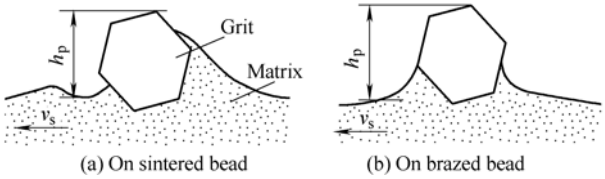

Fig. 6. Protrusive height of the diamond grit

2.3 Tool and workpiece

Brazed beads are fabricated via high-frequency induction heating in a vacuum (<1 mPa), and then, assembled into a wire. The material of spacing tube covers is plastic. The brazing alloys used are Ni-Cr active alloys. The size of diamonds is US mesh 35/40 (d_g ranges from 425 μm to 500 μm and d_{gav} is 462.5 μm). The average diameter of the beads on a wire is usually called the wire diameter (d_w). For the brazed wire, d_w is 7.5 mm and λ_{av} is 60%.

The commercially available sintered wire contains diamonds of 40/45 US mesh size (d_g ranges from 355 μm to 425 μm and d_{gav} is 390 μm) with a 40% concentration. It is sharpened to its steady working stage by sawing firebricks that are commonly used to sharpen impregnated diamond tools. After sharpening, d_w decreases from 7.9 mm to 7.6 mm and λ_{av} reaches 26%, which allows for an excellent cutting rate.

The main properties of a natural marble workpiece are listed in Table 1.

Table 1. Properties of the natural marble workpiece

Main mineral	Particle size	Density ρ/(g • cm^{-3})	Shore hardness HS	Compressive strength σ_{bc}/MPa
Calcite	Pulveryte	2.65	52	93

2.4 Sawing experiments

Sawing experiments are conducted in two feeding modes: constant feed rate feeding (CFF) and constant normal force feeding (CNFF). During the CFF mode, the forces, power and cut depth of the contact curve are measured, whereas during the CNFF mode, the cut depth and cutting time are measured and the feed rate is calculated. The combinations of sawing parameters for CFF and CNFF modes are listed in Tables 2 and 3, respectively. Each combination is repeated five times, and the results are averaged. In the CNFF test, the normal force is adjusted by changing the weight in the sequence '30 N→60 N→90 N'.

Table 2. Sawing parameters for the CFF mode

Sawing length L/mm	Wire speed v_s/(m • s^{-1})	Feed rate v_f/(m • h^{-1})
500	16, 18, 22, 24	0.70
500	20	0.17, 0.45, 0.70, 1.00, 1.25
400, 300	20	0.70

Table 3. Sawing parameters for the CNFF mode

Sawing length L/mm	Normal force F_n/N	Wire speed v_s/(m • s^{-1})
300	30	18, 20, 22
300	60	18, 20, 22
300	90	18, 20, 22

During all these sawing experiments, T_0 is maintained at 3.0 kN. It should be pointed out that the effect of tool wear can be neglected in this study because the total sawing time is very short compared to the wire's service life.

3 Results and Discussion

3.1 Forces

In wire sawing, the bending of the diamond wire in the sawing zone ensures that the diamond grits press into the workpiece to achieve material removal[18]. Considering the large bending radius, the tangential force(F_t) and the normal force(F_n) on the wire can be substituted by F_h and F_v, respectively[19].

The results of the sawing forces(F_t and F_n) versus each of the sawing parameters are plotted in Fig. 7 (BW and SW on all figures in this paper are short for brazed wire and sintered wire, respectively). For the two wires, the tendencies of F_t and F_n versus the sawing parameters are similar. However, under a specific combination of sawing parameters, the brazed wire performs with much lower forces.

The material removal rate(A_q) is the volumetric removal of material per unit time. It is given by the following equation:

$$A_q = d_w v_f L. \tag{1}$$

The relationships of sawing forces to material removal rate are plotted in Fig. 8. The linear relations between sawing force and material removal rate are fitted and

shown on the figure. From the slopes of linear fit lines, it can be calculated that 16% of tangential force and 28% of normal force can be reduced by using the brazed wire compared with those of the sintered wire.

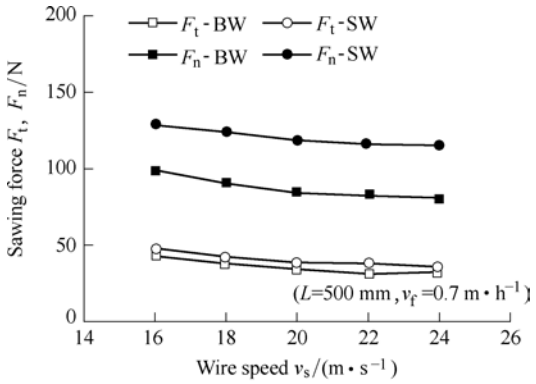

(a) Sawing forces versus wire speed

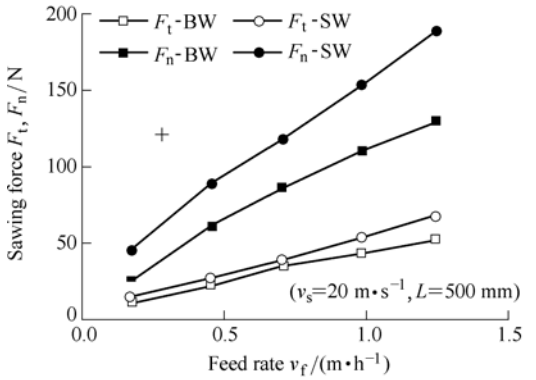

(b) Sawing forces versus feed rate

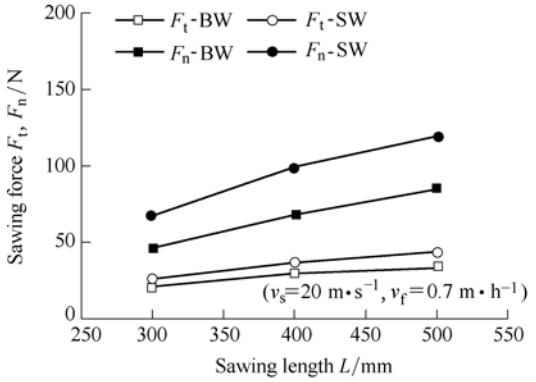

(c) Sawing forces versus sawing length

Fig. 7. Sawing forces versus sawing parameters

Further, the force ratio (F_n/F_t) that is the ratio of normal force to tangential force is calculated and plotted in Fig. 9. It can be seen that F_n/F_t of the brazed wire is 2.3 and it is significantly lower than that of the sintered wire (3.1). It is known that a sharp abrasive tool can exhibit a low force ratio[20]. This implies that the brazed wire is better at cutting into and removing materials, and therefore, performs with significantly lower forces compared to the sintered wire, as addressed above.

3.2 Sawing power

The sawing power is a key index for evaluating the sawing energy efficiency[20]. The power consumed by the two wires versus the material removal rate is plotted in Fig. 10. It is clearly that for each of the two wires its sawing power is nearly linear with the material removal rate.

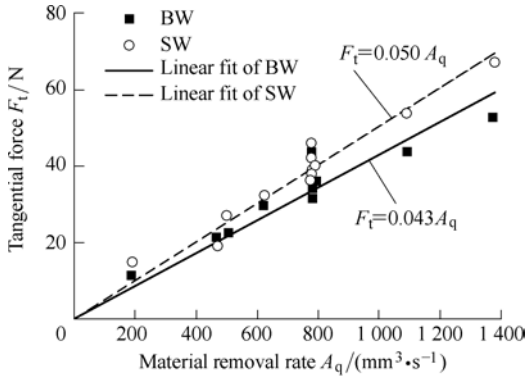

(a) Tangential force versus material removal rate

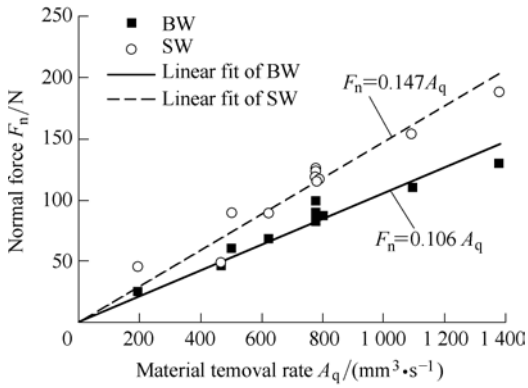

(b) Normal force versus material removal rate

Fig. 8 Sawing forces versus material removal rate

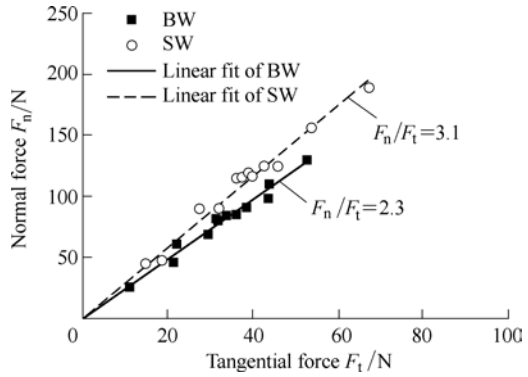

Fig. 9. Force ratio of the two wires

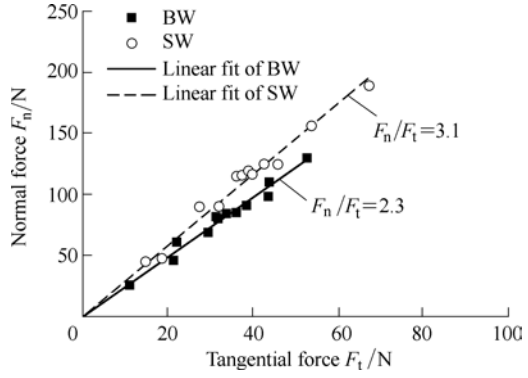

Fig. 10. Sawing power versus material removal rate

Overall, the power consumed by the brazed wire is less than that consumed by the sintered wire. Further, the slopes of the linear relation between power and material removal rate reveals 19% (nearly one-fifth) of sawing power can be reduced by using the brazed wire compared with that of the sintered wire. Therefore, the brazed diamond is preferred over the sintered wire for the green manufacturing.

3.3 Bead topographies

The bead topographies from both the wires are inspected and the results are represented in Fig. 11. For each bead, its holo-photo of a bead is taken from different directions and joined together. From Fig. 10(a), it can be seen that grits on the surface of the sintered bead are randomly distributed. This randomness is inescapable because it is caused by the grits/alloys powder (matrix) mixing process in powder metallurgy sintering. However, from Fig. 10(b), it can be seen that the grits on the brazed bead are uniformly distributed, which is one of the advantages of the brazed diamond. Fig. 12 shows the dispersions of grit protrusions on beads. The protrusions of grits on the sintered bead are scattered, ranging from 10 μm to 250 μm with h_{pav} = 101 μm (standard deviation (S_d) is 48.92). On the other hand, the protrusions of grits on the brazed bead are higher, varying from 250 μm to 325 μm with h_{pav} = 277 μm(S_d = 14.76). λ_{av} of the brazed beads (60%) is significantly greater than that of the sintered beads (26%). Therefore, the protrusions of the grits on the brazed wire are not only much higher but also more uniformly distributed than those on the sintered wire.

(a) Sintered bead

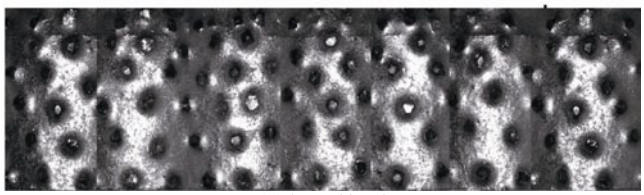

(B) brazed bead

Fig. 11. Holo-photos of diamond beads

For the brazed wire, the combination of the uniform grit order and the high and uniform grit protrusion offers two advantages: increasing the quantity of the active grits engaging in chip formation and reducing the friction effect of chip slurries between the beads and workpiece. It is reported that the friction greatly depends on the chip accommodation space on the bead surface[6, 8]. Fig. 13 illustrates the interactions at the bead/workpiece interface during sawing. For the sintered bead, as shown in Fig. 13(a), the matrix is close to the workpiece surface because of the low girt protrusion rate. This results in insufficient chip accommodation space. Consequently, chips are compressed before leaving the sawing zone. The friction effects of chip slurries at the bead/workpiece interface are greatly increased. From Fig. 13(b), it can be seen that the matrix of the brazed bead can be effectively separated from the workpiece with a large chip accommodation space between the bead matrix and workpiece. This enlarged space is due to the high grit protrusive height and is helpful for chip accommodation. Consequently, the chip friction is greatly reduced. Thus, the preponderance of the brazed bead topography might be responsible for the smaller sawing force and energy consumption exhibited by the brazed wire.

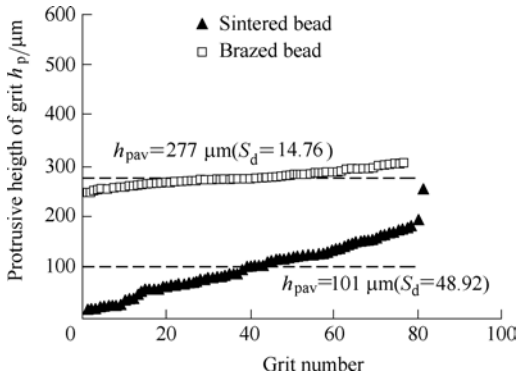

Fig. 12. Dispersions of grit protrusive heights on diamond beads

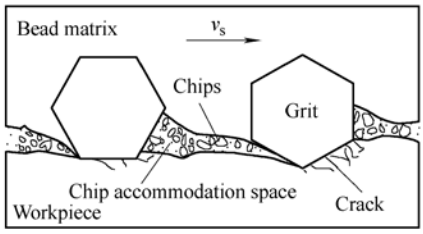

(a) Sintered bead/workpiece

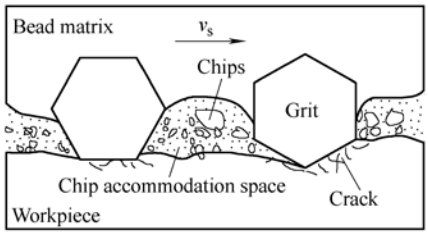

(b) Brazed bead/worpiece

Fig. 13. Interactions at the bead/workpiece interface during sawing

3.4 Contact curve linearity

In wire sawing, the bending of the diamond wire in the sawing zone ensures that diamond grits press on the workpiece, thereby removing material[18]. As a result, the contact curve at the wire/workpiece interface is not straight. It is known that the bending of the contact curve prevents

high dimensional accuracy, particularly in profile sawing. In fact, this is the same key problem in wire electrical discharge machining (WEDM).

The degree of linearity of the contact curve can be represented by the deviation from the different contact curve positions (ΔD_c), which can be calculated as follows:

$$\Delta D_c = D_{cmin} - D_c, \tag{2}$$

where D_{cmin} is the minimum cut depth on the contact curve.

Fig. 14 represents the deviations from the different contact curve positions during the steady sawing stage for which the cutting parameters are the same. It is clear that the linearity of the contact curve of the brazed wire is better than that of the sintered wire. For wire sawing, the bending level of the wire is positively related to its normal force[18]. The improved linearity might be attributed to the low normal force acting on the brazed wire (see Fig. 6). On the basis of this improved linearity, the brazed wire is preferable over the sintered wire for profile sawing.

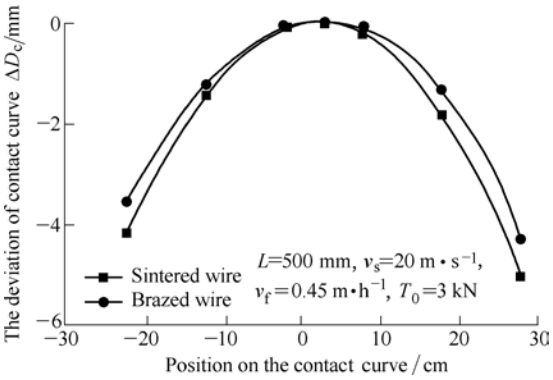

Fig. 14. Deviation of contact curve in steady sawing

3.5 Sawing efficiency

The sawing efficiency (sawing rate) for wire sawing is commonly assessed by the feed rate. Under the CNFF mode, the feed rate is calculated by dividing the cut depth by the cutting time. Fig. 15 shows feed rates calculated under different sawing conditions. The feed rates of the brazed and sintered wires increase with the normal force and wire speed, respectively. However, for a specific combination of sawing parameters, the brazed wire has nearly two times the feed rate of the sintered wire. From Eq. 2, it clearly follows that the material removal rate is doubled when using the brazed wire. This outcome supports the results mentioned above. The smaller F_n/F_t and the bead topography superiority allow the brazed bead to cut into the workpiece much more easily. Meanwhile, the larger λ_{av} of the brazed bead also provides adequate chip accommodation space for chip slurries. Therefore, the cutting ability of the brazed wire is greatly enhanced and the sawing rate is doubled.

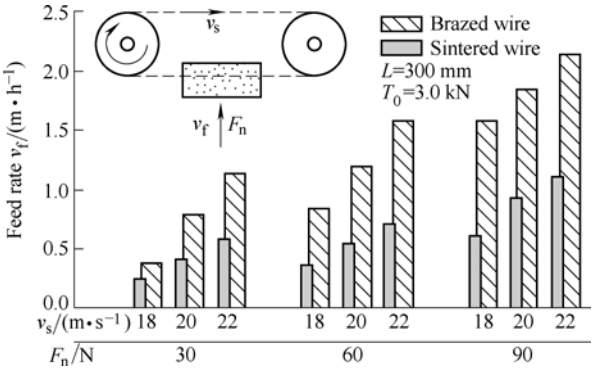

Fig. 15. Feed rates of the two wires in the CNFF test

4 Conclusions

(1) The brazed diamond wire exhibits with lower sawing forces compared to the sintered wire: 16% of tangential force and 28% of normal force can be reduced.

(2) The force ratio of the brazed diamond wire is lower than that of the sintered wire. This means that the brazed wire is sharper than the sintered wire and cuts into workpiece much more easily.

(3) The brazed diamond wire consumes less power than the sintered diamond wire. The linear fit between power and material rate reveals that nearly one-fifth of power can be saved by using the brazed wire.

(4) The contact curve linearity during cutting with a brazed wire is better than that with a sintered wire because of the smaller normal sawing force acting on the brazed wire.

(5) the sawing production rate can be doubled by using the brazed wire compared to the sintered wire.

References

[1] DAVIS P R. The future of diamond abrasives in stone processing[J]. *Industrial Diamond Review*, 2001, 61(3): 159–167.

[2] WRIGHT D N, ENGELS J A. The environment and cost benefits of using diamond wire for quarrying and processing of natural stone[J]. *Industrial Diamond Review*, 2003, 63(4): 165–24.

[3] MOLFINO R M, ZOPPI M. A robotic system for underwater eco–sustainable wire-cutting[J]. *Automation in Construction*, 2012, 24(3): 213–223.

[4] HUANG Guoqin, XU Xipeng. Analysis of the breakage of diamond wire saws in sawing of stone[J]. *Key Engineering Materials*, 2006, 304–305: 123–126.

[5] HUANG Hui, XU Xipeng. Study on the wear of diamond beads in wire sawing[J]. *Materials Science Forum*, 2006, 532–533: 436–439.

[6] ÖZÇELIK Y, BAYRAM F. Optical investigations of bead wear in diamond wire cutting[J]. *Industrial Diamond Review*, 2004, 64(3): 60–65.

[7] ÖZÇELIK Y, KULAKSIZ S, CETIN M C. Assessment of the wearing on diamond beads in the cutting of different rock types by the ridge regression[J]. *Journal of Materials Processing Technology*, 2002, 127(3): 392–400.

[8] TÖNSHOFF H K, ASCHE J. Wear of metal-bond diamond tools in the machining of stone[J]. *Industrial Diamond Review*, 1997, 57(1): 7–13.

[9] HUANG Guoqin, HUANG Hui, GUO Hua, et al. Influences of sawing parameters on forces and energy in wire sawing of granite[J]. *Journal of Mechanical Engineering*, 2009, 43(3): 234–239. (in

Chinese)

[10] OLIVEIRA L J, BOBROVNITCHII G S, FILGUEIRA M. Processing and characterization of impregnated diamond cutting tools using a ferrous metal matrix[J]. *International Journal of Refractory Metals & Hard Materials*, 2007, 25(4): 328–335.

[11] RISSO L, VICENZI B, BERNIERI S. Improved cutting performance of diamond beads by means of innovative shape [C] // *Proceedings of the Second International Industrial Diamond Conference*, Rome, Italy, April 19–20, 2007: B.1.1.

[12] ÖZÇELIK, Y. Optimum working conditions of diamond wire cutting machines in the marble industry[J]. *Industrial Diamond Review*, 2005, 1(5): 58–64.

[13] ÖZÇELIK, Y. Development of a single diamond bead test machine for marble cutting[J]. *Industrial Diamond Review*, 2008, 68(1): 56–62.

[14] CHATTOPADHYAY A K, CHOLLET L, HINTERMANN H E. Experimental investigation on induction brazing of diamond with Ni-Cr hardfacing alloy under argon atmosphere[J]. *Journal of Materials Science*, 1991, 26(18): 5 093–5 100.

[15] SUNG J C, SUNG M. The brazing of diamond[J]. *International Journal of Refractory Metals and Hard Materials*, 2009, 27(2): 382–393.

[16] SUNG C M. Brazed diamond grid: a revolutionary design for diamond saws[J]. *Diamond and Related Materials*, 1999, (8): 1 540–1 543.

[17] XIAO Bing, FU Yucan, SU Honghua, et al. Machining performance of brazed diamond wire saw with optimum grain distribution[J]. *Key Engineering Materials*, 2005, 304–305: 43–47.

[18] LIU B C, ZHANG Z P, SUN Y H. Sawing trajectory and mechanism of diamond wire saw[J]. *Key Engineering Materials*, 2004, 259–260: 395–400.

[19] NAKAGAWA H B, NAKAZWA H D, NISHIMURA N K, et al. High-speed and high-accuracy slabbing of marble using diamond wire saw[J]. *Journal of Japanese Social Abrasive Technology*, 2004, 48(6): 329–334 (in Japanese).

[20] MALKIN S. *Grinding technology: theory and applications of machining with abrasives*[M]. New York: American Society of Civil Engineers, 1989.

Biographical notes

HUANG Guoqin, born in 1981, is currently a lecturer at *Huaqiao University, China*. From there he received his PhD degree in 2010. His research interests include the fabrication of super-abrasive tools, high efficiency cutting, modelling, and the optimization of abrasive machining.
Tel: +86–592–6162359; E-mail: smarthgq@hqu.edu.cn

XU Xipeng, born in 1964, is currently a professor and a PhD candidate supervisor at *Huaqiao University, China*. He received his PhD degree at *Nanjing University of Aeronautics and Astronautics, China*, in 1992. He worked as a visiting researcher at the *Grinding Research Laboratory*, *University of Massachusetts, United States of American*, from 1998 to 1999. His research interests include machining and grinding processes for hard and brittle materials, tribology issues in machining with abrasives, and the fabrication of super-abrasive tools.
E-mail: xpxu@hqu.edu.cn